

# Automatic Webcam-Based Human Heart Rate Measurements Using Laplacian Eigenmap

Lan Wei<sup>1</sup>, Yonghong Tian<sup>1,\*</sup>, Yaowei Wang<sup>2</sup>, Touradj Ebrahimi<sup>3</sup>,  
and Tiejun Huang<sup>1</sup>

<sup>1</sup> National Engineering Lab for Video Technology, Peking University

<sup>2</sup> Department of Electronics Engineering, Beijing Institute of Technology  
yhtian@pku.edu.cn

<sup>3</sup> Swiss Federal Institute of Technology

**Abstract.** Non-contact, long-term monitoring human heart rate is of great importance to home health care. Recent studies show that Photoplethysmography (PPG) can provide a means of heart rate measurement by detecting blood volume pulse (BVP) in human face. However, most of existing methods use linear analysis method to uncover the underlying BVP, which may be not quite adequate for physiological signals. They also lack rigorous mathematical and physiological models for the subsequent heart rate calculation. In this paper, we present a novel webcam-based heart rate measurement method using Laplacian Eigenmap (LE). Usually, the webcam captures the PPG signal mixed with other sources of fluctuations in light. Thus exactly separating the PPG signal from the collected data is crucial for heart rate measurement. In our method, more accurate BVP can be extracted by applying LE to efficiently discover the embedding ties of PPG with the nonlinear mixed data. We also operate effective data filtering on BVP and get heart rate based on the calculation of interbeat intervals (IBIs). Experimental results show that LE obtains higher degrees of agreement with measurements using finger blood oximetry than Independent Component Analysis (ICA), Principal Component Analysis (PCA) and other five alternative methods. Moreover, filtering and processing on IBIs are proved to increase the measuring accuracy in experiments.

## 1 Introduction

Usually, medical instruments supporting contact measurements (*e.g.* electrocardiogram, arm blood pressure monitor and auscultoscope) bring much discomfort to patients in constant monitoring. One possible approach to overcome the contact with skin is to use webcam to collect the PPG signal for measurements. PPG is a photoelectric technology of detecting the blood volume changing in living tissues. It provides the information of BVP that propagates throughout the body, which can be used for heart rate extraction. Based on this idea, Ming-Zher Poh *et al.* tried to apply ICA on video images of human face to extract

---

\* Corresponding author.

underlying BVP for cardiac pulse rate measurement [1]. Similarly, Magdalena Lewandowska obtained heart rate directly from webcam with PCA [2]. According to the Beer-Lambert law, reflected light intensity traveled through facial tissue varies nonlinearly with distance. Neither ICA nor PCA could extract the pure BVP from collected data, as both of them are based on linear hypothesis.

This paper proposes a novel webcam-based method to measure human heart rate using LE [3]. In our approach, the red, green, and blue (RGB) color sensors of webcam collect the changing signal of reflected light intensity on human face. The source signal is a mixture of BVP along with other sources of fluctuations in light. As LE is a *manifold learning* method using for uncovering the inner structure of data, we apply LE to extract BVP from the collected signal. Then we do some simple but effective data processing with the extracted BVP, and get heart rate based on the calculation of IBIs. The step of extracting BVP from signal source counts much, which is also a process of dimensionality reduction for raw data. PCA [4], Linear Discriminant Analysis (LDA) [5] and ICA [6] are classic linear dimensionality reduction methods. In addition, manifold learning methods proposed in recent years, such as Isomap [7], Locally Linear Embedding (LLE) [8], LE, Local Tangent Space Alignment (LTSA) [9], Maximum Variance Unfolding (MVU) [10], and Linearity Preserving Projection (LPP) [11] can also be used for dimensionality reduction. All of these methods could also be applied for the BVP extraction in our application. Through the comparison of nine dimensionality reduction methods: Isomap, LLE, LE, LTSA, MVU, LPP, PCA, LDA and ICA, it reaches a conclusion that LE generates the best results.

*Our contributions are as follows:*

1. We use LE to extract BVP from video images of human faces.
2. We propose a robust heart rate calculation method based on IBIs calculation from the desired BVP.
3. We do extensive experiments on other eight alternative methods: Isomap, LLE, LTSA, MVU, LPP, PCA, ICA and LDA, and give the conclusion that LE is a reasonable choice for this application.

The rest of the paper is organized as follows: Section 2 puts forward some related work. Section 3 introduces the heart rate extraction model based on LE. Section 4 shows the results of experiments compared with other alternative methods. Section 5 presents the conclusion.

## 2 Related Work

PPG is a non-invasive photoelectric means of detecting the changes in blood volume of living tissue [12]. The basic clinical application of PPG technology is blood saturation measurements [13]. In 1996, Nakajima *et al.* successfully used the PPG collected at the earlobe to extract heart rate [14]. Johansson designed a heart rate and respiratory rate detection system based on PPG in 1999. They also used it to monitor new-borns for up to eight hours [15]. Aoyagi and Miyasaka in 2002 extracted the oxygen saturation (SpO<sub>2</sub>) and heart rate information through

PPG [16]. Making use of the pulse transit time in human body, PPG technology could also be used for blood pressure measurements [17].

Pavlidis and colleagues proposed the idea of continuous monitoring human physiological conditions based on human face information in 2003 [18]. They made attempts to the non-contact measurements of human facial blood flow, heart pulse rate and respiratory rate using thermal camera [19,20,21]. They proposed the concept of "*desktop health monitoring*" and established a human-computer interaction system in 2007. The system was composed of computer and thermal camera, and provided the support of monitoring a full range of physiological signs [20]. Jia Zheng *et al.* set up a remote PPG synchronous imaging system using a camera, and put forward a proposal of 3D blood microcirculation model for physiological conditions assessment based on it [22].

2010, Ming-Zher Poh *et al.* adopt ICA for separating the ordinary face video data collected by webcam and successfully recovered cardiac pulse [1]. ICA is a technique of blind source separation for uncovering the independent source signals from a set of data which is composed of linear mixtures of the underlying sources. It was once applied to reduce motion artifacts in PPG measurements [24]. In further research, Ming-Zher Poh used a webcam to restore the human heart rate variability (HRV), discharge cycle, respiratory rate and other physiological indicators [23]. It proved that ICA tolerated motion artifacts well for measurements. 2011, Magdalena Lewandowska *et al.* tried to use PCA to extract the changeable component of data collected by webcam to measure heart rate [2]. By comparing the cardiac pulse signal obtained by PCA and ICA, they gave a conclusion that those two methods had similar accuracy and PCA was a better choice for less computationally complex. They also tested the effects of setting small rectangular regions of interest (ROI) of the face image and only two color channels. However, both ICA and PCA are linear data analysis methods. To the best of our knowledge, no studies so far have attempted to use nonlinearity methods, to say nothing of manifold learning methods, for heart rate extraction.

### 3 The Proposed Method

Image sequences of human face contain the information of BVP for heart rate extraction. With this idea, we apply LE for BVP extraction and set up the heart rate measurement system. The system contains the modules of face detection, continuous measurements, results displaying and timer (Fig. 1). Face detector detects faces in video images collected from webcam (or media files). Averages of each RGB channels are saved continuously in background. After a period of collection, the three-dimensional RGB data is put into LE and the algorithm outputs the mapping data in one-dimensional space, which is the desired BVP signal. After some data processing procedures, system gets heart rate.

#### 3.1 Laplacian Eigenmap

LE, which is based on spectral graph theory, makes use of the Laplacian-Beltrami operator in manifold to get the mapping of high-dimensional onto low-dimensional

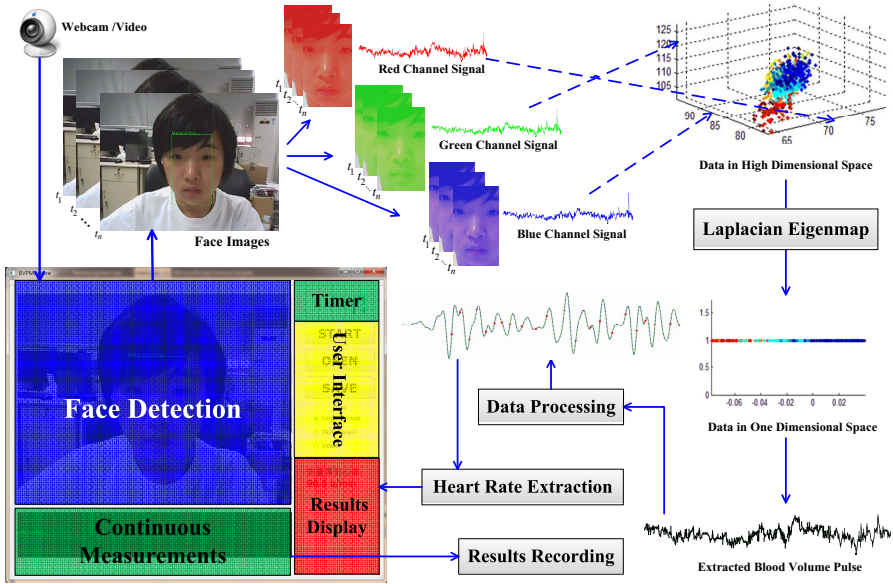


Fig. 1. System architecture

space. It aims at discovering the embedded low-dimensional data set in low-dimensional space while maintaining the distance relation of any two points [3,25]. In this paper, we apply LE in heart rate measurements to extract the underlying BVP signal from images of human face.

We utilize a free Open Computer Vision (OpenCV) library (Version 2.3.1) to get the region of the face in the video images. The face detector in OpenCV known as "Haar detector" is first proposed by Paul Viola and Michael Jones [26] and extended with Haar-like characteristics by Rainer Lienhart and Jochen Maydt [27]. The ROI rectangle is defined as the central 60% of the width and full height of the rectangle containing the face region. As the experiment is for single person, we always take the face with the largest area when detector detects more than one face; if the detector fails to find a face, we copy the detection results of the last frame.

All pixels in RGB channels of the ROI are averaged separately for each frame. For the  $i$ th frame image, we save the vector:

$$X_i(j) = (x_1(j), x_2(j), \dots, x_n(j)) \quad j = 1, 2, 3$$

where  $x_i(1)$ ,  $x_i(2)$  and  $x_i(3)$  separately represents the averages of the pixels in RGB channel in  $i$ th frame. We consider  $X_i$  as a point in three dimensional space. The aim of LE is to find the mapping onto one-dimensional space  $Y = (y_1, y_2, \dots, y_n)$  of  $X = (x_1, x_2, \dots, x_n)^3$ .

Firstly, it calculates the Euclidean distance of the input matrix  $X$  to get the square matrix  $G$ . Edges of the graph stand for the adjacent relationship between

nodes. Nodes  $i$  and  $j$  on  $G$  are adjacent if  $i$  is among  $k$  nearest neighbors of  $j$  or  $j$  is among  $k$  nearest neighbors of  $i$  [3]. The key of LE is to solve the following optimization problem:

$$\min \sum_{ij=1}^n \|y_i - y_j\|^2 W_{ij} . \tag{1}$$

here weight  $W_{ij}$  is the proximate measure of two near points  $x_i$  and  $x_j$ . Under normal conditions, the closer  $x_i$  and  $x_j$  gets, the larger the value of  $W_{ij}$  is. As a result, when they are mapped onto low-dimensional space,  $y_i$  and  $y_j$  would also be close. By computing the generalized eigenvectors of the Figure Laplace matrix, it gets the embedded low-dimensional of the data.

*The algorithmic steps of LE are as follow in Fig. 2 :*

```

1. Construct the adjacent graph  $G$ 
   Define  $k = 12$ ;
   for ( $i = 1; i < n; i ++$ )
       if ( $x_j$  is one of the  $k$  most recent points of  $x_i$ )
            $x_i$  and  $x_j$  are considered to be adjacent;
2. Calculate the weights matrix  $W_{ij}$ 
   if ( $x_i$  and  $x_j$  are adjacent)
        $w_{ij} = 1$ ;
   else
        $w_{ij} = 0$ ;
3. Get the Low-dimensional embedding  $Y$ 
   Divide  $G$  into connected part graphs  $G = \{G_1, G_2, \dots, G_m\}$ ;
   for ( $i = 1; i < m; i ++$ )
        $D_{ii} = \sum_i W_{ji}$ ;
        $L = D - W$ ;
       Solve the equation  $Ly = \lambda Dy$  to get  $Y_i$ ;
    $Y = [Y_1, Y_2, \dots, Y_m]$ 
    
```

**Fig. 2.** The algorithmic steps of LE

The extracted BVP with LE in one experiment is shown in Fig. 3.

### 3.2 Heart Rate Extraction

Data processing is performed to reduce the measurements errors. The first pre-processing operation is to remove the singular points. Here we define "singular points" as the points which are greater than (or less than) 10 times of the average. After the removal, we use the average of two adjacent points to interpolate the vacant position. In addition, as there may be a larger error at the very start of measurement caused by shaking or initialization of face detector, we directly remove the data collected within first second. Then *moving average filter* is

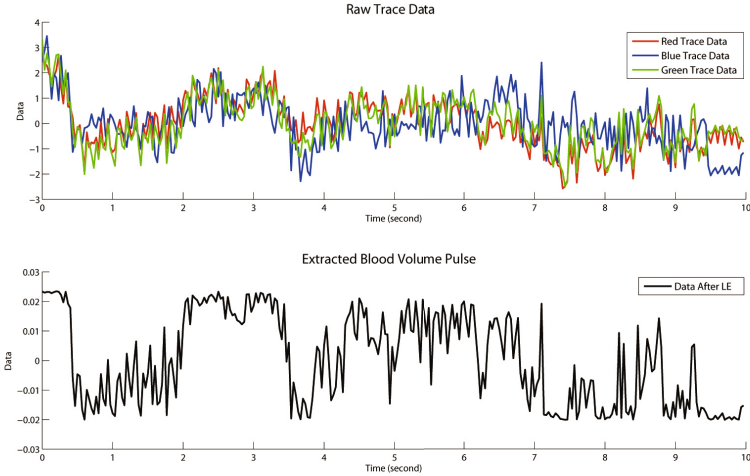


**Fig. 3.** Raw trace data and extracted BVP

used to smooth the curve, suppressing the sharp noise. For the BVP signal  $Y = [y_1, y_2, \dots, y_n]$ , the average filter is described as:

$$y'_i = \frac{1}{M} \int_{k=i-(M+1)/2}^{k+(M-1)/2} y(k) . \tag{2}$$

$i$  is from  $(M + 1)/2 + 1$  to  $N - (M - 1)/2 + 1$ ,  $M$  is the moving point and  $M = 5$ .

*Band-pass filter* is needed to process the glitches in high-frequency and noise in low-frequency. We use 15-point Hamming window, 0.7 - 4 Hz cut-off frequency, band-pass filter to smooth the data. Two common methods can be used for heart rate extraction: One uses power spectral density function; and the other is to make use of the periodic interval time  $T$  between two adjacent BVP waveforms, which is IBIs. In order to speed up the calculation, as well as make it easy for continuous measurement, we use the second method based on IBIs to get heart rate. We choose the first-order differential point in each cycle of BVP as characteristic point to demarcate the interval. The number of first-order differential points in a period of wave fluctuates narrowly than the number of usual maximum points in the presence of measuring errors. *Cubic spline interpolation* is applied to the data for ensuring the existence of continuous first-order differential and second-order differential. Then average interval time is calculated as follow:

$$\bar{T} = \frac{\sum_{k=2}^n t_k - t_{k-1}}{k - 1} . \tag{3}$$

$m$  is the number of feature points in the sampling interval. We consider the interval between  $[0.25, 2]$  (corresponding to heart rate is 30 - 240bpm) as effective

interval. If  $t_k - t_{k-1}$  is larger than 2, we consider it as two time intervals; If  $t_k - t_{k-1}$  is less than 0.25s, we merge it with the next time interval (discard it if it's the last interval). In the end, we get the heart rate value:

$$f_{HR} = 60/\overline{T} . \quad (4)$$

Fig. 4 shows the results after each step of data processing, as well as the final first-order differential characteristic points for IBIs calculation.

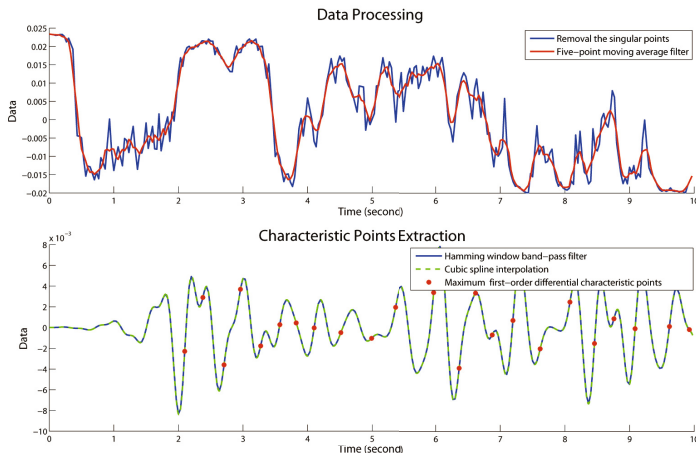


Fig. 4. Data processing results and the characteristic points

## 4 Experiments and Results

### 4.1 Experimental Setup

The experimental setup was made up of a basic webcam (Logitech C170) externally connected to a desktop computer (Dell Optiplex 790) and a finger pulse oximetry (Contec CMS50D-Plus, 30 250bpm range) (Fig. 5). The video images of participants faces were recorded while they sit in front of the computer. In each experiment, 30 seconds long video sequences in colour (24-bit RGB with 3 channels 8 bits/channel) were recorded and saved as AVI format (compressed with MJPG codec type) on the computer. The resolution of the videos was 640x480 pixels and the frame rate was 30 frames per second (fps). While recording, the finger pulse oximetry measured the heart rate synchronously at a sampling rate of 1Hz. The experiments were conducted indoors. 20 participants (11 males and 9 females) aging from 20 to 80 took the experiments.

Participants were asked to be sitting naturally in our experiments and slight movement is tolerated. Paper [1] did experiments to prove ICA tolerates motion artifacts. While in practice the illumination variations have a larger influence

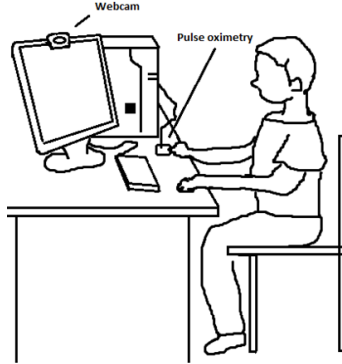


Fig. 5. Experimental setup

on the performance than motion artifacts. So we did two sets of experiments with different illumination variations. Each participant recorded two videos of 30 seconds long per each. For the first video, we used sunlight as the only source of illumination. Then spot light (SamvoL 6W High Power Spotlights 01b) was used as light source for the second set of videos.

#### 4.2 Heart Rate Measurements Using Different Methods

We took data collected in 10 seconds as the initial processing unit. Subsequent measurements were performed using a 10s moving window with one second increment (90% overlap). Measurements of the finger blood oximetry in every 10 seconds were averaged as contrast. Each experiment continued for 30 seconds, yielding 21 results.

We performed the measurements with other eight dimensionality reduction methods. Five manifold learning method: Isomap, LLE, LTSA, MVU, LPP, and three linear dimensionality reduction method: PCA, LDA and ICA. After doing

Table 1. Measurements of 20 participants with different illumination

Algorithm	Experiment using sunlight			Experiment using spot light			Average Time(s)
	Mean	+1.96SD	-1.96SD	Mean	+1.96SD	-1.96SD	
Isomap	-10.8	27.7	-49.4	-23.6	2.9	-50.1	1.7073
LLE	-2.0	6.7	-10.6	-1.9	4.8	-8.5	0.2308
LE	-0.3	1.2	-2.6	-0.1	0.6	-1.9	0.1393
LTSA	-1.8	6.3	-9.8	-1.9	5.4	-9.2	0.3199
MVU	8.79	10.37	7.20	8.59	10.07	7.10	1.2065
LPP	-1.8	6.3	-9.8	-1.9	5.4	-9.2	0.0996
PCA	3.5	12.9	-6.0	-0.4	8.0	-1.96	0.0321
LDA	-3.3	5.2	-11.8	-5.7	2.8	-14.1	0.0029
ICA	-2.9	-1.3	-4.5	-2.2	0.9	-5.3	0.5065



40 sets of experiments (20 sets use sunlight and 20 sets use spotlight ) with each algorithm, we exhibited the Bland-Altman plots of each with the results of finger blood oximetry to demonstrate the methods' effect in continuous measurements (see Table 1 and Fig. 6). It was obvious that LE, whose mean error was -0.1 b/min with 95% limits of agreement +0.6 to -1.9 b/min when used spotlight, obtained higher degrees of agreement with measurements using finger blood oximetry.

As shown in the table, Isomap turns out to be the last choice. Other manifold learning methods, such as LLE, LE, LTSA, LPP seems to be more reliable than the linear methods. But the better results are at the expense of much execution time. In some experiments, MVU fails to output results as neighborhood graph struttred by collected data may be not connected, causing a maximization of a function without upper bound.

Results of LLE and LPP are shown in strip-like patterns. This is because the step of reconstructing data point in LLE makes the data lose its time tag. The final results of LLE fall into a small range after filtration.(In contrast, other methods may get quite different results for each person.) As a person's heart rate changed little in 30s, measurements of each person are divided in regions. Data fluctuating in time shaft seems like an oblique line in B-A plot. LPP is the linear version of LLE. They get similar results as the data set is simple.

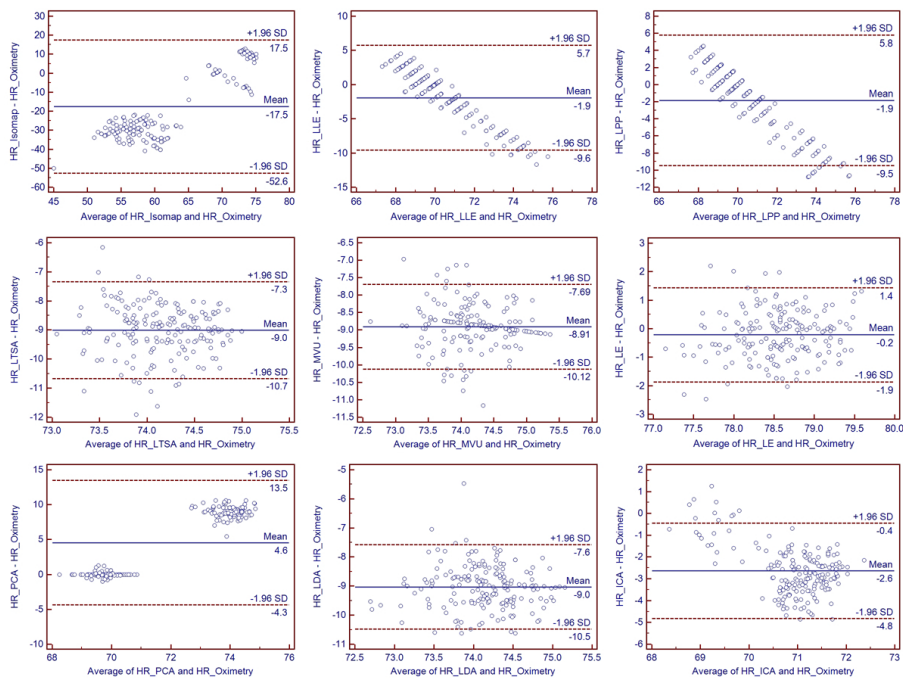


**Fig. 6.** Bland-Altman plots for each dimensionality reduction method with the measurements of finger blood oximetry

PCA is effectual sometimes, but its results have great volatility depending on the lighting conditions of the experiment. LDA aims at making the output data have good separability after dimensionality reduction. So it gets poor agreement with ground truth when the collected data has great error, especially movement artifact. ICA separates data into three independent components, and the choice of the independent components affects results. In addition, it gets the separating results by stopping iteration when it fails to get optimal solution, which spends a lot of time. All in all, LE is the advisable choice for the proposed application.

### 4.3 Heart Rate Measurements Without Data Processing

Still utilizing LE for BVP extraction, we did experiments using maximum points for IBIs calculation. Moreover, we abandoned the data processing of singular points removal, average filtering, band-pass filtering and process for interval.

Data in one experiment was shown in Fig. 7. The number of characteristic points increased a lot as the narrow fluctuations caused by error were considered to be interval, which would have a negative effect on results.

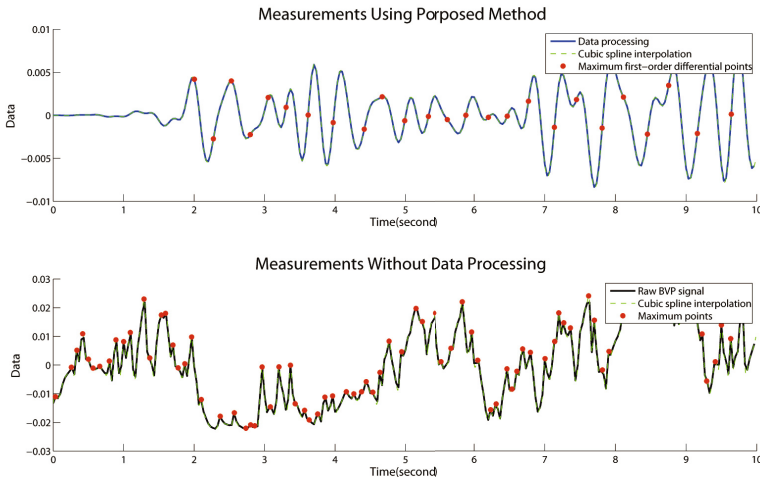


**Fig. 7.** Measurements using proposed method and without data processing

Two Bland-Altman plots demonstrating the agreement between measurements obtained from the tested method and from finger blood oximetry were shown in Fig. 8. With the proposed method, mean error was  $-0.2$  b/min with 95% limits of agreement  $+1.4$  to  $-1.9$  b/min. Without data processing of singular points removal, average filtering, band-pass filtering, the points were distributed distant from zero, and mean error was  $+149.1$  with 95% limits of agreement  $+170.3$  to  $+127.9$  b/min. It proved that data filtering and processing on IBIs did increase the measuring accuracy a lot.

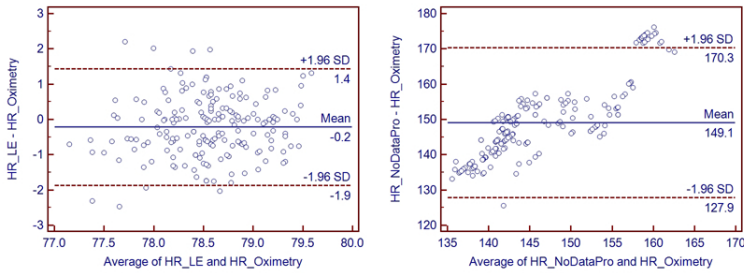


**Fig. 8.** Bland-Altman plots of measurements using the proposed method and measurements without data processing

## 5 Conclusion

In this paper, we present a novel method for webcam-based continuous non-contact heart rate measurement using Laplacian Eigenmap. The results of 20 participants demonstrate the advantage of our approach compared with other eight dimensionality reduction methods. The following data processing is also proved to be necessary. The presented technology is reliable, easy to use, and promising for extending and improving daily monitoring of home health care. Further studies may be performed on other human physiological signs, such as respiratory rate and blood pressure through many other channels, such as remote medical care or mobile terminals.

**Acknowledgement.** This work was supported in part by grants from International Science & Technology Cooperation Program of China under Contract 2010DFA31520, and in part by the Chinese National Natural Science Foundation under Contract No. 60973055, No. 61035001, and No. 61072095.

## References

1. Poh, M.Z., McDuff, D.J., Picard, R.W.: Non-contact, automated cardiac pulse measurements using video imaging and blind source separation. *Opt. Express*, 10762–10774 (2010)
2. Lewandowska, M., Rumiski, J., Kocejko, T.: Measuring pulse rate with a webcam - a non-contact method for evaluating cardiac activity. In: *Computer Science and Information Systems (FedCSIS)*, pp. 18–21 (2011)
3. Belkin, M., Niyogi, P.: Laplacian eigenmaps for dimensionality reduction and data representation. *Neural Computation* 15, 1373–1396 (2003)
4. Shlens, J.: A tutorial on principal component analysis. Institute for Nonlinear Science, UCSD (2005)
5. Mika, S., Ratsch, G., Weston, J., Scholkopf, B., Mullers, K.R.: Fisher discriminant analysis with kernels. *Neural Networks for Signal Processing IX*, 41–48
6. Comon, P.: Independent component analysis: a new concept? *Signal Processing* 36, 287–314 (1994)

7. Tenenbaum, J., De Silva, V., Langofrd, J.: A global geomertic framework for non-linear dimension reduction. *Science*, 2319–2323 (2000)
8. Roweis, S.T., Saul, L.K.: Nonlinear dimensionality reduction by locally linear embedding. *Science* 5500, 2323–2326 (2000)
9. Zhang, Z., Zha, H.: Principal manifolds and nonlinear dimensionality reduction by local tangent space alignment. *SIAM Journal Scientific Computing*, 313–338 (2004)
10. Weinberger, K., Saul, L.: Unsupervised learning of image manifolds by semidefinite programming. *Int. J. Comp. Vision*, 11–90 (2006)
11. He, X., Niyogi, P.: Locality preserving projections. In: *Proc. Conf. Advances in Neural Information Processing Systems* (2003)
12. Challoner, A.V.J.: Photoelectric plethysmography for estimating cutaneous blood flow non-invasive physiological measurements, vol. 125. Academic Press (1979)
13. Webster, J.G.: *Design of pulse oximeters*. Institute of Physics Publishing, Bristol (1997)
14. Nakajima, K., Tamura, T., Miike, H.: Monitoring of heart and respiratory rates by photoplethysmography using a digital filtering technique. *Med. Eng. Phys.*, 365–372 (1996)
15. Johansson, A., Oberg, P.A.: Estimation of respiratory volumes from the photoplethysmographic signal. *Med. Biol. Eng. Comput.*, 42–47 (1999)
16. Aoyagi, T., Miyasaka, K.: Pulse oximetry: its invention, contribution to medicine, and future tasks. *Anesth. Analg.*, S1–S3 (2002)
17. Naschitz, J.E., et al.: Pulse transit time by r-wave-gated infrared photoplethysmography: review of the literature and personal experience. *Clin. Monit. Comput.*, 333–342 (2004)
18. Garbey, M., Merla, A., Pavlidis, I.: Estimation of blood flow speed and vessel location from thermal video. In: *Proceedings of the IEEE Computer Society Conference on Computer Vision and Pattern Recognition*, pp. 356–363 (2004)
19. Sun, N., Garbey, M., Merla, A.: I Pavlidis: Imaging the cardiovascular pulse. In: *IEEE Computer Society Conference on Computer Vision and Pattern Recognition* (2005)
20. Pavlidis, I., Dowdall, J., Sun, N., Puri, C., Fei, J., Garbey, M.: Interacting with human physiology. *Comput., Vis., Image Underst.* 108 (2007)
21. Fei, Pavlidis, I.: Thermistor at a distance: unobtrusive measurement of breathing. *IEEE Trans. Biomed. Eng.* 57, 988–998 (2010)
22. Zheng, J., Hu, S., Azorin-Peris, V., Echiadi, A.: Remote simultaneous dual wavelength imaging photoplethysmography: a further step towards 3-d mapping of skin blood microcirculation. In: *Proc. of SPIE*, vol. 206, pp. 159–178 (2008)
23. Jianchu, Y., Warren, S.: A short study to assess the potential of independent component analysis for motion artifact separation in wearable pulse oximeter signals. In: *IEEE Conference of the Engineering in Medicine and Biology Society*, pp. 3585–3588 (2005)
24. Poh, M.Z., McDuff, D.J., Picard, R.W.: Advancements in noncontact, multiparameter physiological measurements using a webcam. *IEEE Trans. Biomed. Eng.* (2011)
25. Belkin, M., Niyogi, P.: Laplacian eigenmaps and spectral techniques for embedding and clustering, pp. 585–591. MIT Press, MA (2001)
26. Viola, P., Jones, M.: Rapid object detection using a boosted cascade of simple features. In: *Proceedings of the International Conference on Computer Vision and Pattern Recognition*, vol. 1, pp. 1063–6919 (2001)
27. Lienhart, R., Maydt, J.: An extended set of haar-like features for rapid object detection. In: *Proceedings of the IEEE Conference on Image Processing*, pp. 900–903 (2002)